9th INTERNATIONAL SYMPOSIUM ON MEASUREMENT AND QUALITY CONTROL (9th ISMQC)
November 21 – 24, 2007, IIT Madras

TWO WAVELENGTH MICROSCOPIC TV INTERFEROMETRIC SYSTEM FOR SURFACE PROFILING

Paul Kumar U., Basanta Bhaduri, Krishna Mohan N. Kothiyal, M. P.
Applied Optics Laboratory, Department of Physics
Indian Institute of Technology Madras, Chennai - 600 036
E-mail : paul@physics.iitm.ac.in

Abstract: *Non-contact techniques for rapid and accurate mapping of micro-machined surfaces are important for the optoelectronic industry. Interferometry is an important tool for precision metrology of surfaces. It has been used for applications such as surface profiling, roughness measurement and quality testing of optical elements. The single-wavelength conventional interferometry can handle the smoothly varying surface profiles and step-heights less than half a wavelength. In this paper we describe a two wavelength microscopic TV interferometric system which removes ambiguity associated with the single wavelength data and also extends the phase measurement range compared to the conventional single wavelength interferometry. The results obtained using this two wavelength microscopic system for 3D surface profiling on smooth specimens are presented.*

Key words: *Two wavelength microscopic TV interferometry, phase reversal subtraction technique, phase shifting, surface profiling, fringe analysis.*

1. INTRODUCTION

Interferometry has been used for applications such as surface profiling, deformation, roughness measurement and quality testing of optical elements. 3D surface profile of an object is essential for the complete deformation studies where a careful analysis of sensitive vector orientation across the field-of-view is necessary for reliable quantitative measurements. The conventional interferometric profilers using a single wavelength offer excellent vertical resolution, but a serious limitation to their use is that they can only handle smooth profiles and step heights less than half a wavelength. The approaches adopted to overcome the problem of small dynamic range are based on two or multi-wavelength interferometry (Cheng & Wyant, 1984; Creath, 1987; Schmit & Hariharan, 2006; North-Morris, et.al., 2004) and white light interferometry (Chim & Kino, 1990; Chim & Kino, 1991; Chim & Kino, 1992; Deck & de Groot, 1994; de Groot & Deck, 1995; de Groot et.al., 2002). Careful choice of wavelengths enables the system to make use of long range measurements. If the phase of the surface under test is measured at two wavelengths, λ_1 and λ_2, then the difference between the two corresponds to the modulo-2π phase map that could have been generated with a longer wavelength given by the relation $\lambda_{eff}=\lambda_1\lambda_2/|\lambda_1-\lambda_2|$ (Creath, 1987). By combining the two-wavelength interferometry with the phase shifting it is possible to obtain the dynamic range of the effective wavelength for 3D surface profiling. We describe a two wavelength microscopic TV interferometric system using a Thales-Optem 125C long working distance (LDM) zoom module. Further, we demonstrate a phase reversal subtraction (PRS) technique that yields high contrast and noise reduced fringe pattern for analysis. The phase reversal addition-subtraction techniques are widely implemented for applications such as optical image subtraction (Ebersole, 1975; Venkateswara Rao & Krishna Mohan 2002), phase shift calibration and phase measurement (Suja Helen et.al., 1998). The addition of π phase shifted images eliminates the fringe modulation (Suja Helen et.al., 1998), while the subtraction of the same removes the unwanted background noise to yield high contrast fringes (Yatagai, 1993). For phase extraction at each wavelength, we have used the phase reversal subtracted five phase shifted images using a five step algorithm (Hariharan et al., 1987). The experimental results for surface profiling pertaining to step height evaluation on smooth specimens are presented.

2. TWO WAVELENGTH MICROSCOPIC TV INTERFEROMETRY

Fig. 1 represents the schematic a microscopic TV interfrometric system with frequency doubled Nd:YAG (λ_1=532nm,50mW) and He-Ne (λ_2=632.8nm, 20mW) lasers. Both the beams are expanded and collimated using a spatial filtering setup (SF) and a 150 mm focal length collimating lens (CL). An iris in front of the lens allows to adjust the size of the collimated beam, while the variable neutral density filters (VND) in the setup helps to control intensity of the beams. Shutters S_1 and S_2 in front of the lasers allow to switch over from one wavelength to other wavelength. The collimated laser beam illuminates the specimen under study and a reference mirror via a beam splitter (BS) simultaneously. The specimen is mounted on a 3-axes translation stage for alignment. The microscopic imaging system consists of a Thales-Optem zoom 125C long working distancemicroscope (LDM) with an extended zoom range and a Sony 2/3" CCD camera (XC-ST70CE). The Zoom LDM provides a 12.5:1 zoom ratio, at working

distance of 89 mm with 1.0X objective. The resolution of the CCD is 752(H) x 582(V) pixels and the size of each pixel is 11.6μm x 11.2μm respectively. The reflected beams from the specimen and the smooth reference mirror for each wavelength are recombined coherently onto the CCD plane to yield interference fringe pattern via the same beam splitter and the microscopic imaging system. The CCD camera is interfaced to PC with NI1409 card. A PZT (STr 25/150/6PZT from Piezomechanik) driven reference mirror is used for introducing the phase shifts between the object and reference beams. It is interfaced to a PC with a DAQ card (NI6036E). The process of image acquisition with phase shifting at each wavelength is carried out with the support of software in LabVIEW.

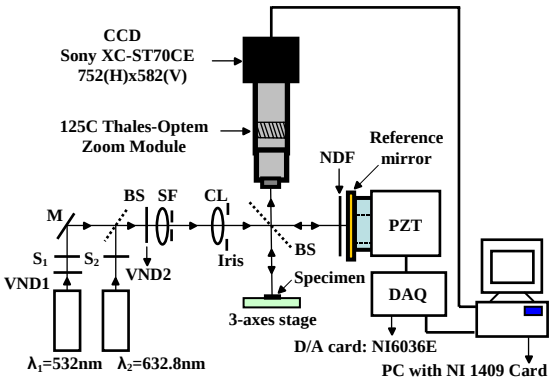

Fig.1 Schematic of a two wavelength microscopic TV interferometric system: S_1 , S_2 Shutters; VND, Variable neutral density filter; M, Mirror; BS, Beam splitter; SF, Spatial filter; CL, Collimating lens; NDF, neutral density filter; DAQ, Data acquisition system.

3. THEORY

For incorporating the proposed phase reversal subtraction (PRS) technique for 3D surface profiling we store separately seven π/2 phase shifted frames at each wavelength λ_i (i=1,2). Assuming that the intensities of reflected object and reference waves are same for each wavelength, one can express the total intensity distribution of the seven phase shifted frames for each wavelength λ_i as

$$I_{in} = I_O + I_R + 2\sqrt{I_O I_R}\cos(\phi_i + (n-1)\frac{\pi}{2}) \qquad (1)$$

Where, I_O and I_R are the intensities of the object and reference beams respectively, ϕ_i is the phase corresponds to wavelength λ_i (i = 1, 2), and n is the number of the phase shifted frames (n = 1 to 7). The phase can be extracted from the stored phase shifted frames by adopting five, seven or proposed phase reversal subtraction (PRS) five phase step algorithms as given below:

(i) Five phase step algorithm

Phase distribution ϕ_i corresponding to λ_i using the five phase step algorithm (Hariharan et al., 1987) can be obtained from

$$\phi_i^5 = \arctan\left(\frac{2(I_{i2} - I_{i4})}{2I_{i3} - I_{i1} - I_{i5}}\right) \qquad (2)$$

(ii) *Seven phase step algorithm*

Phase distribution ϕ_i corresponding to λ_i using the seven phase step algorithm (de Groot, 1995) can be obtained from

$$\phi_i^7 = \arctan\left(\frac{-I_{i1} + 7I_{i3} - 7I_{i5} + I_{i7}}{-4I_{i2} + 8I_{i4} - 4I_{i6}}\right) \qquad (3)$$

(iii) *Phase reversal subtraction (PRS) five phase step algorithm*

For incorporating the phase reversal subtraction technique from the stored seven π/2 phase shifted frames as shown in Eq. (1), we first generate the five phase reversal subtraction frames by subtracting the frames with phase shift 0 and π, π /2 and 3π /2, π and 2π, 3π /2 and 5π /2, 2π and 3π . The intensity of these five phase reversal subtraction frames can be written as

$$\begin{aligned} I'_{i1} &= 4\sqrt{I_O I_R}\,[\cos\phi_i] \\ I'_{i2} &= -4\sqrt{I_O I_R}\,[\sin\phi_i] \\ I'_{i3} &= -4\sqrt{I_O I_R}\,[\cos\phi_i] \\ I'_{i4} &= 4\sqrt{I_O I_R}\,[\sin\phi_i] \\ I'_{i5} &= 4\sqrt{I_O I_R}\,[\cos\phi_i] \end{aligned} \qquad (4)$$

The phase distribution ϕ_i for each wavelength from the five PRS frames as given in Eq. (4) can now be obtained as

$$\phi_i^{PRS5} = \arctan\left(\frac{2(I'_{i2} - I'_{i4})}{2I'_{i3} - I'_{i1} - I'_{i5}}\right) \qquad (5)$$

We have found that the phase maps obtained from the PRS five step algorithm yield noise reduced phase maps compared to the conventional phase map extraction method using directly either five or seven phase step algorithm given in Eq. (2) and Eq. (3) respectively.

The evaluated phase ϕ_i is wrapped between $-\pi$ to π due to arctangent function. The unambiguous range of single wavelength can be extended by subtracting measured phases at two different wavelengths

$$\phi_{eff} = \phi_1 - \phi_2 \qquad (6)$$

Where, ϕ_1 and ϕ_2 are independently measured phases at λ_1 and λ_2 respectively and ϕ_{eff} is the phase measured at the effective wavelength λ_{eff} which is give by the relation (Creath, 1987)

$$\lambda_{eff} = \frac{\lambda_1 \lambda_2}{|\lambda_1 - \lambda_2|} \quad (7)$$

In case of optical profilers, the 3D surface profile depth or height 'Z' can be obtained from the relation

$$Z = \frac{\phi_{eff}}{4\pi} \lambda_{eff} \quad (8)$$

4. 3D SURFACE PROFILING

Surface profiling at effective wavelength λ_{eff} = 3.34μm is carried out by subtracting the individual phases measured at λ_1=532nm and λ_2=632.8nm respectively. The experiments were conducted on a smooth silicon sample with a step. The reflected beams from the specimen and the reference mirror for each wavelength interfere at the CCD and one can observe a fringe pattern on the TV monitor. Initially the PZT was calibrated for both the wavelengths independently for storing the π/2 phase shifted fringe patterns. For each wavelength seven π/2 phase shifted frames are stored with the support of LabVIEW and the alternative fringe patterns that are π phase shifted are subtracted in sequential order to yield high contrast noise reduced five phase shifted fringe patterns at each wavelength for analysis. Fig. 2(a) and Fig. 2(b) represent the initial and π phase shifted fringe patterns along with the line scan along the central x-axis. Fig. 2(c) represents the subtracted fringe pattern which is noticeably less noisy than the individual fringe patterns. Following the procedure described above, we have generated the phase reversal subtracted five phase shifted fringe patterns for each wavelength. The wrapped phase maps obtained at λ_1=532nm and λ_2=632.8nm using the Eq. (5) are shown in Fig. 3(a) and Fig. 3(b) respectively. When the wrapped phase at λ_1=532nm is subtracted from the wrapped phase at λ_2=632.8nm, the result is the wrapped phase shown in Fig. 3(c) which is effectively measured at λ_{eff} = 3.34μm (Eq. (7)). The phase map shown in Fig. 3(c) is then unwrapped. The resultant 2D and 3D profiles after removing the tilt are shown in Fig. 3(d) and Fig. 3(e) respectively. Fig. 3(f) provides the line scan surface profile along the central x-axis. The height of the step has been determined by linear least square fitting across the top and bottom of the profile and determining the height difference at the location of the step. From the analysis the measured step height is 130nm. This step height can as well be evaluated from the phase maps of individual wavelengths λ_1 and λ_2 unambiguously. The values obtained are 130nm and 130nm for λ_1 and λ_2 respectively. This agreement with the two wavelength process shows proper working of our two wavelength set-up.

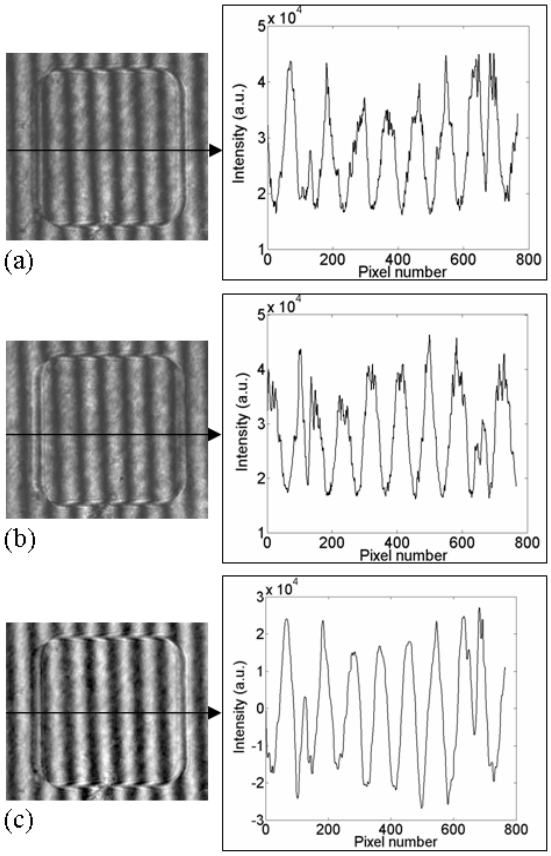

Fig.2. The interferograms at λ_1 =532nm along with the line scan along the central x-axis (a) initial pattern, I_{11}, (b) π phase shifted pattern, I_{13} and (c) phase reversal subtraction pattern , I_{11} - I_{13}.

The technique is also applied on a silicon sample with large step. The systematic analysis carried out for step height measurement is shown in Fig. 4. From the analysis the measured step height is 645nm. This value agrees well with the result on same sample by white light interferometry (Debnath et al., 2003).

We have extended the surface profile analysis to a MEMS pressure sensor of a 1.5mm^2 square silicon membrane with thickness of 108μm on a silicon wafer of 480μm thickness. The reflective sensor is placed on a 3-axes stage and aligned with reference to the optically flat reference mirror to obtain a fringe free field at the CCD plane. However, a step between the membrane and the silicon wafer results in a fringe pattern. Fig. 5(a) and Fig. 5(b) show typical phase reversal subtraction interferograms at each wavelength. Fig. 5(c) and Fig. 5(d) represent the corresponding wrapped phase maps while Fig. 5(e) shows the subtraction between the two phase maps. Fig. 5(f) and Fig. 5(g) are the 2D and 3D surface profiles of the MEMS pressure sensor. Fig.5 (h) shows a scan across the diaphragm. It is seen that the silicon membrane is projected out around 1.6μm with reference to the silicon wafer.

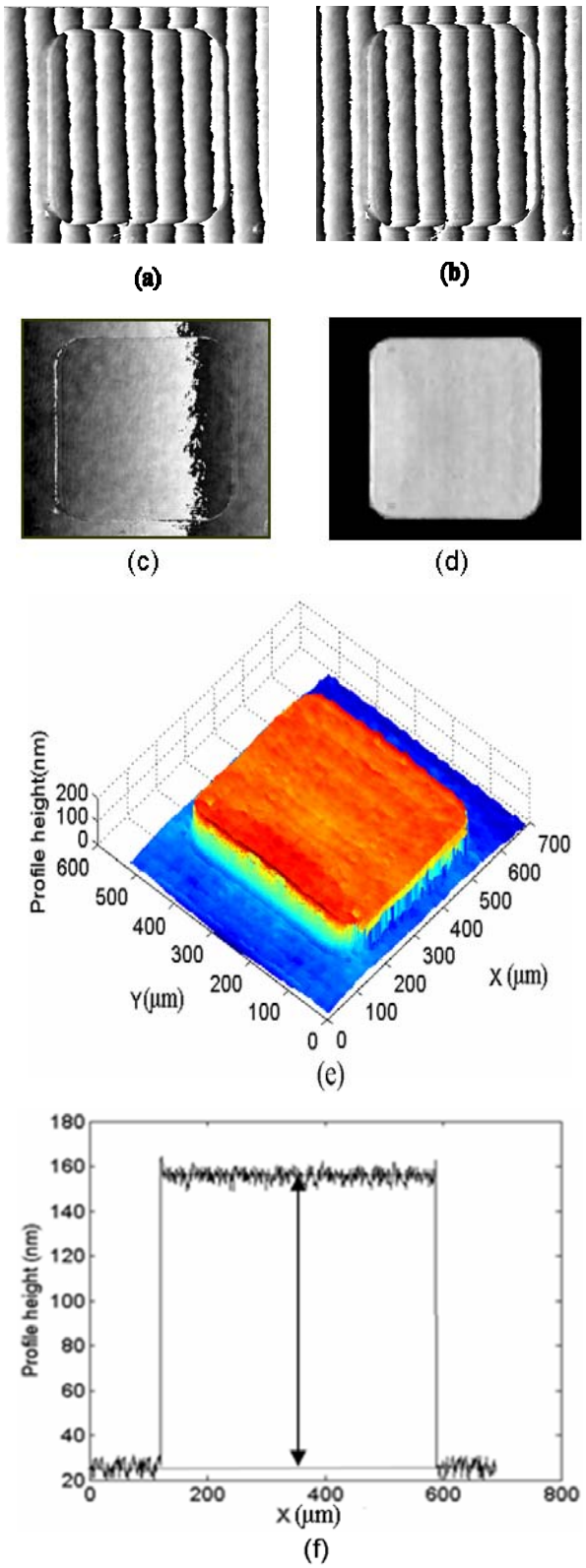

Fig.3. Step height measurement on a silicon sample (a) wrapped phase map at 532 nm, (b) wrapped phase map at 632.8nm, (c) wrapped phase map at effective wavelength, 3.34µm, (d) 2D profile, (e) 3D profile and (f) step height profile line scan along the central x-axis.

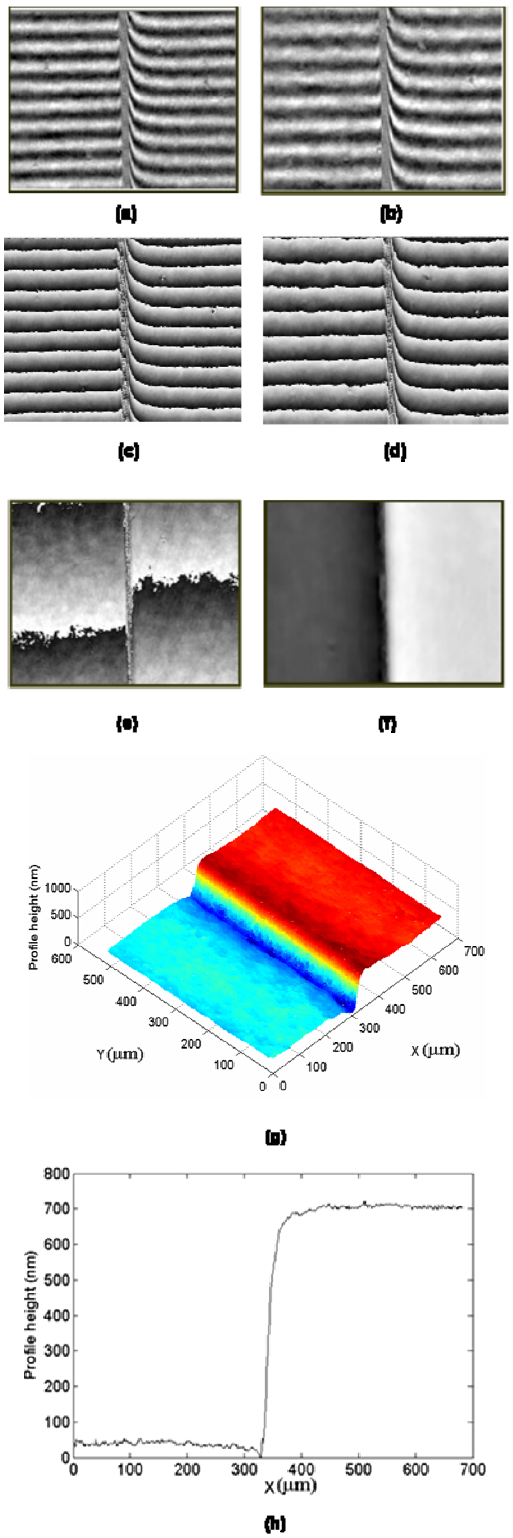

Fig.4. Measurement on a silicon sample with large step (a) phase reversal subtraction interferogram at 532 nm, (b) phase reversal subtraction interferogram at 632.8nm, (c) Phase map at 532 nm, (d) phase map at 632.8nm, (e) phase map at effective wavelength, 3.34µm, (f) 2D profile, (g) 3D profile and (h) step height profile line scan along the central x-axis.

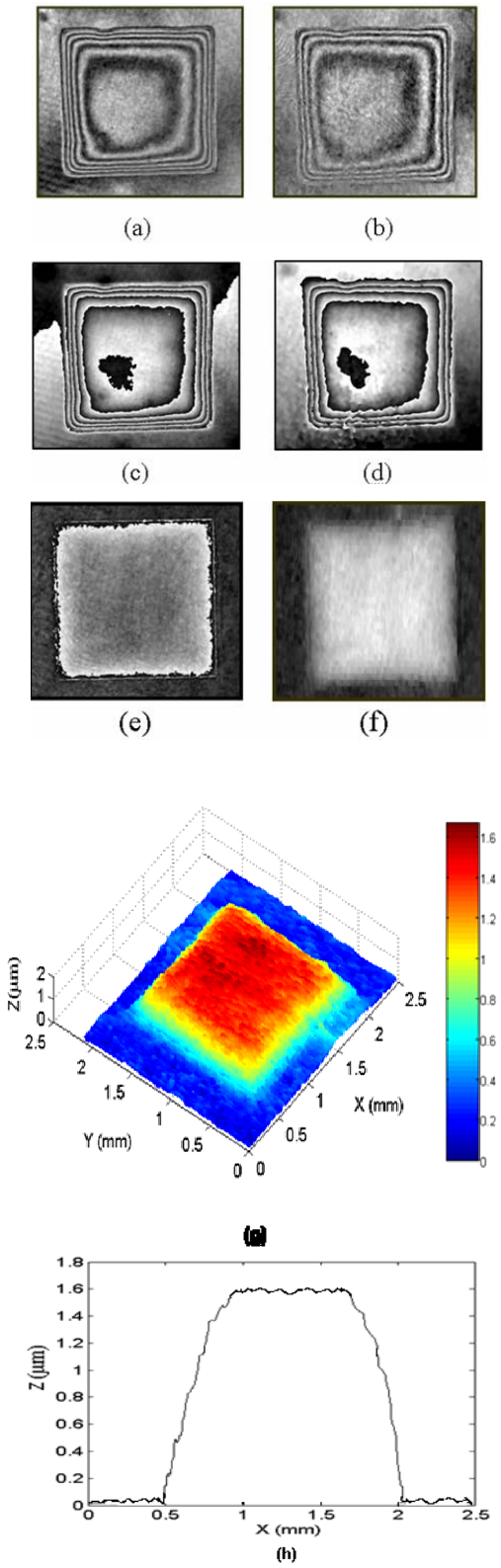

Fig.5. Surface profiling on a MEMS pressure sensor (a) phase reversal subtraction interferogram at 532 nm, (b) phase reversal subtraction interferogram at 632.8nm, (c) Phase map at 532 nm, (d) phase map at 632.8nm, (e) phase map at effective wavelength, 3.34µm, (f) 2D profile, (g) 3D profile, and (h) profile line scan along the central x-axis.

5. CONCLUSIONS

Two wavelength microscopic TV interferometric system using a long working distance zoom module is developed and demonstrated for 3D surface profiling. The setup can be used for smooth or rough specimens. Two-wavelength sequential illumination technique makes it possible to overcome the problem of ambiguities associated with single wavelength data which is adequate for many purposes. A phase reversal subtraction (PRS) five phase step algorithm for obtaining the absolute phase data with reduced noise is also described. A number of specimens for 3D surface profiling are investigated to show the function and reliability of the developed two wavelength microscopic interferometric system. Application of the system to study the profile silicon based MEMS pressure sensor is presented.

6. ACKNOWLEDGEMENT

This work is supported by *Defense Research and Development Organization* (DRDO).

7. REFERENCES

Cheng, Y. Y. & Wyant, J. C. (1984). Two wavelength phase shifting interferometry, *Applied Optics*, Vol. 23, pp. 4539-4543.

Creath, K. (1987). Step height measurement using two-wavelength phase-shifting interferometry, *Applied Optics*, Vol. 26, pp. 2810-16.

Chim, S. S. C. & Kino, G. S. (1990). Correlation microscope. *Optics Letters*, Vol. 15, pp. 579-581.

Chim, S. S. C. & Kino, G. S. (1991). Phase measurement using the Mirau correlation microscope, *Applied Optics*, Vol. 30, pp. 2197-2201.

Chim, S. S. C. & Kino, G. S. (1992). Three dimensional image realization in interference microscopy, *Applied Optics*, Vol. 31, pp. 2550-2253.

Dale, M.; Buckberry, C. & Towers, D. (2000). Two wavelength contouring for shape and deformation measurement, *Proceedings of SPIE*, Vol. 4076, pp.181-190.

de Groot, P. (1995). Derivation of algorithms for phase-shifting interferometry using the concept of a data-sampling window, *Applied Optics,* Vol. 34, pp. 4723-4730.

de Groot, P. & Deck, L. (1995). Surface profiling by analysis of white-light interferograms in the spatial frequency domain, *Journal of Modern Optics,* Vol. 42, pp. 389-401.

de Groot, P.; de Lega, X. C.; Kramer, J. & Turzhitsky, M. (2002). Determination of fringe order in white-light interference microscopy. *Applied Optics*, Vol. 41, pp. 4571-4578.

Debnath, S. K.; Senthil, R.; Shanthi, P.; Sharma, D. K. & Kothiyal, M. P. (2003). Use of PZT phase shifter in the analysis of spectrally resolved white light interferogram, *Proceedings of International*

Conference on Laser Applications and Optical Metrology (ICLAOM-03), Shaker, C & Mehta, D. S. (Eds.), Dec. 1-4, Anamaya Publishers, New Delhi, pp. 241-244.

Deck, L. & de Groot, P. (1994). High speed noncontact profilier based on scanning white light interferometry, *Applied Optics*, Vol. 33, pp.7334-7338.

Ebersole, J. E. (1975). Optical image subtraction, *Optical Engineering,* Vol. 14, pp. 436-447.

Hariharan, P.; Oreb, B. F. & Eiju, T. (1987). Digital phase shifting interferometry – a simple error-compensating phase calculation algorithm. *Applied Optics,* Vol. 26, pp. 2504-2506.

North-Morris, M. B.; Millerd, J. E. Brock, N. J. & Hayes, J. B. (2004). Phase shifting multi-wave length dynamic interferometry, *Proceedings of SPIE*, Vol. 5531, pp. 64-75.

Schmit, J. & Hariharan, P. (2006). Two-wavelength interferometry profilometry with a phase-step error-compensating algorithm, *Optical Engineering*, 45, pp. 115602-1-115602-3.

Suja Helen, S.; Ara, M. H.; Darlin, J. S.; Krishna Mohan, N.; Kothiyal, M. P. & Sirohi, R. S. (1998). Phase step calibration and phase measurement in image plane holography using $BaTiO_3$ crystal as recording medium, *Optical Engineering*, Vol. 37, pp. 2918-2925.

Venkateswara Rao, V. & Krishna Mohan, N. (2002). Optical image processing phase reversal Twyman-Green interferometer. *Proc. of SPIE*, Vol. 4736, pp.184 -188.

Yatagai, T.(1993). Intensity based analysis methods, in: *Interferogram analysis,* Robinson, D. W. & Reid, G. T. (Eds.) Chapter 3, pp. 72-93, Institute of Physics Publishing, London.